Journal of Zhejiang University-SCIENCE A (Applied Physics & Engineering)
ISSN 1673-565X (Print); ISSN 1862-1775 (Online)
www.zju.edu.cn/jzus; www.springerlink.com
E-mail: jzus@zju.edu.cn

Monitoring rapid urban expansion using a multi-temporal RGB-impervious surface model*

Amirreza SHAHTAHMASSEBI[†1], Zhou-lu YU[1], Ke WANG[†‡1], Hong-wei XU[1], Jin-song DENG[1], Jia-dan LI[1], Rui-sen LUO[1], Jing WU[1], Nathan MOORE[1,2]

([1]*Institute of Agriculture Remote Sensing and Information Technology, Zhejiang University, Hangzhou 310029, China*)
([2]*Department of Geography, Michigan State University, MI 48823, USA*)
[†]E-mail: amir511@zju.edu.cn; kwang@zju.edu.cn

Received Feb. 15, 2011; Revision accepted Aug. 17, 2011; Crosschecked Dec. 29, 2011

Abstract: In this paper, we developed a novel method of combining remote sensing tools at the sub-pixel level for accurate identification of impervious surface time series changes. We examined the use of the red-green-blue impervious surface model (RGB-IS) in detecting time series internal modification of urban regions by integrating Landsat data collected over four different periods between 1987 and 2009 (i.e., 1987, 2000, 2002, and 2009). The performance of this approach was compared with two conventional methods, namely standard RGB-normalized difference vegetation index (NDVI) and post-classification technique. In contrast to conventional techniques, RGB-IS could monitor between-class changes, within-class changes, and location of these modifications. The proposed method was independent of seasonal changes and was also able to serve as a useful alternative for quick mapping growth hotspots and updating transportation corridor map. The results also showed that Cixi County, Zhejiang Province, China experienced tremendous impervious surface changes, especially along the corridors of newly constructed highways and around urban areas over the past 22 years.

Key words: Red-green-blue impervious surface model (RGB-IS), Multi-temporal, Impervious surface, Landsat
doi:10.1631/jzus.A1100034 **Document code:** A **CLC number:** TP79

1 Introduction

Since China commenced economic reforms and the Open Door Policy in 1978, tremendous land-use change has occurred, particularly in many coastal regions of China (Long *et al*., 2007), such as Hangzhou Bay (Ding *et al*., 2007). For the development of the Hangzhou Bay region, the Chinese government has provided strong financial and infrastructure support; for example, constructing Hangzhou Bay Bridge, highways, high speed railways, and industrial zones. While Hangzhou Bay is going through rapid development, it is facing a range of environmental risks, among which, rapid land cover and land use change (LCLUC) is one of the most important problems.

Evaluating the impacts of urban growth in Hangzhou Bay has long been a focus of many recent research projects (Ramadan *et al*., 2004; Lu *et al*., S.L., 2006; Ding *et al*., 2007; Deng *et al*., 2009). These studies used common change-detection methods, including image-to-image comparison and map-to-map comparison. Despite distinct advantages of these methods, several limitations are recognized. First, the majority of these studies used remotely sensed data, assuming homogeneity within a single pixel, resulting in no quantifiable changes at the sub-pixel level (Yang *et al*., 2003b). However, urban landscapes are typically composed of features that are

‡ Corresponding author
* Project (No. 2006BAJ05A02) supported by the National Science and Technology Pillar Program during the 11th Five-Year Plan Period of China

smaller than the spatial resolution of most medium spatial resolution sensors, such as Landsat pixels. As a result, ignoring the sub-pixel variation of Landsat imagery can lead to a biased estimate in urban change analysis (Yang *et al.*, 2003b). Second, change detection based on image classifications, no matter how detailed, can only quantify between-class conversion but not within-class modification or intensification, and thus can provide an incomplete trajectory of urban landscape dynamics (Yang and Liu, 2005). Finally, conventional classification techniques may not be appropriate for extracting characteristics of urban regions (Powell *et al.*, 2007). For example, the physical composition of land use classes may vary dramatically from region to region due to different building materials and different construction practices, thereby limiting cross-regional comparisons between urban areas (Small, 2005). In rapidly growing cities, particularly in the developing world, multiple forms of land use may occur within the same geographic space, limiting the usefulness of traditional land use urban categories (Powell *et al.*, 2007). Nevertheless, in recent years, advance techniques, such as impervious surface estimation, have reinforced and expanded the applicability of remote sensing data to the urban change detection context.

Impervious surface describes the whole of non-water permeable surfaces including roads, buildings, parking lots, railways, and side walks (Esch *et al.*, 2009). The amount of impervious surface in a landscape is an important indicator of environmental and habitat quality (Arnold and Gibbons, 1996). This index has shown a promising use for identifying the pattern and intensity of urban growth, because the percentage of imperviousness is likely related to the major urban land cover types and their changes. Change detection based on impervious surface not only captures urban extent, but also provides spatially explicit information concerning the direction and magnitude of change in built-up land covers (Powell *et al.*, 2007).

Numerous methodologies have been introduced to extract impervious surface and monitor urban changes (Klein, 1979; Yang *et al.*, 2003a; Lu and Weng, 2006; Weng, 2007). These techniques include regression tree and decision tree (Yang *et al.*, 2003a; Dougherty *et al.*, 2004), stepwise multivariate statistic model (Yang, 2006), self-organizing map and multi-layer perceptron (Lee and Lathrop, 2006; Chormanski *et al.*, 2008; Hu and Weng, 2009), fuzzy technique (Lizarazo and Barros, 2010), expert system (Mountrakis *et al.*, 2009), multisource and hybrid classification (Luo and Mountrakis, 2010; Mountrakis and Luo, 2011), and spectral mixture analysis (Rashed *et al.*, 2005; Lu and Weng, 2006; Li *et al.*, 2010).

More recent studies have adopted the multiple endmember spectral mixture analysis (MESMA) technique to estimate impervious surface (Powell *et al.*, 2007; Rashed, 2008; Franke *et al.*, 2009). MESMA allows the number and type of endmemebers to vary on a per-pixel basis (Powell *et al.*, 2007). Rashed (2008) described MESMA as a modified linear spectral mixture analysis (SMA) approach in which many simple SMA models are first calculated for each pixel in the image. Then the objective is to choose, for every pixel in the image, which model among the candidate models provides the best fit to the pixel spectrum while producing physically reasonable fractions (Roberts *et al.*, 1998).

Most impervious surface change detection analysis methods based on either MESMA or other techniques, have mainly focused on two dates of satellite images or more than two dates of imagery using dates comparison in sequence (Powell *et al.*, 2008; Rashed, 2008) rather than a composite analysis of three dates as multi-temporal data. This situation worsens if more than three time series remote sensing data are used for urban land cover change detection, especially for detection of between-class and within-class urban changes. It is imperative to design some new methods that can be used effectively to monitor time series dynamic change of urban land use/cover at the sub-pixel level.

Previously, Sader and Winne (1992) successfully demonstrated the potential of using color composite red-green-blue-normalized difference vegetation index (RGB-NDVI) based on the additive color theory to map forest area change at three dates. The RGB-NDVI change detection technique was found to be accurate and efficient compared to other methods, such as image differencing. This is because when determining change, RGB-NDVI incorporated three dates at one time as opposed to two-date stepwise sequences using image differencing methods.

It is particularly advantageous when time series images (e.g., four) are analyzed in a sequence to detect changes (Sader *et al*., 2001). The RGB-NDVI technique may also have some predictive potential for future area changes given the sequence of change activities and new road building.

In this paper, we expand the traditional RGB-NDVI technique (Sader and Winne, 1992; Sader *et al*., 2003) by developing a methodology to map variation of imperviousness change at four dates, namely RGB-impervious surface model (RGB-IS). Note that impervious surface was estimated by using the MESMA technique. The design and development of the RGB-IS technique specifically focus on a number of criteria to achieve this study. The method should (1) map between-class and within-class urban modifications at three points of time or a composite analysis of three dates as a multi-temporal dataset; (2) recognize location of between-class and within-class changes; (3) quickly monitor the impervious surface changes in large and rapid urbanization regions; and (4) be automate or semi-automate and be easy to understand, particularly for those in the field of urban and land use planning. The results of RGB-IS are also compared with the traditional RGB-NDVI and post-classification techniques, for disadvantages and improvements. Moreover, we validate the proposed algorithm in a case study, a rapidly growing county (Cixi County) located at Hangzhou Bay, Zhejiang Province, China.

2 Study area

Cixi County lies in the central part of the golden economic triangle formed by Shanghai, Hangzhou, and Ningbo (Fig. 1). Since the economic reforms of the 1980s in China, Cixi County has made enormous achievements of socio-economic development. In 2005, among more than 2000 counties and cities in China, the socio-economic development composite index of this County ranks the 14th. It is one of the top four counties in Zhejiang Province. Cixi County's gross domestic product (GDP) increased rapidly from 2.42 billion RMB in 1987 to 62.6 billion RMB in 2009. Concomitant with significant economic development and industrialization, and tremendous immigration, Cixi County has witnessed a rapid urbanization process and experienced fundamental land use change in the last decade. To some extent, Cixi County represents the economic-developed regions undergoing a typical urbanization process throughout the Hangzhou Bay region.

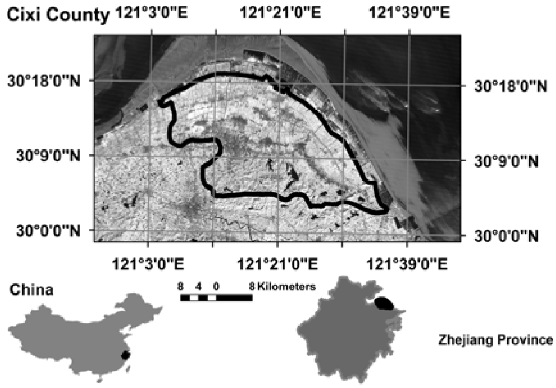

Fig. 1 Location of this study

3 Methodologies

As shown in Fig. 2, the proposed methodology consists of six sequential phases: (1) impervious surface separately estimated from individual images using the MESMA technique; (2) NDVI separately computed for each image; (3) RGB model applied to impervious surface fractions and NDVI images; (4) change detection process including applying decision tree classifier (DTC) to RGB-IS and iterative self-organizing data analysis (ISO-DATA) to RGB-NDVI; (5) post-classification; and (6) change analysis and comparison.

3.1 Data preprocessing

Landsat thematic mapper (TM) and enhanced TM plus (ETM+) data were used as the primary data source for imperviousness mapping and change detection. The predominately cloud free images of Landsat imagery covering Hangzhou Bay were obtained for 1987, 2000, 2002, and 2009 (Table 1).

These images have already been accurately rectified and geo-referenced to a pixel size of 30 m on a universal transverse Mercator (UTM) map projection (Zone 51) with the World Geodetic System 1984 datum. The dark object correction method was applied to each band. The method is as effective as

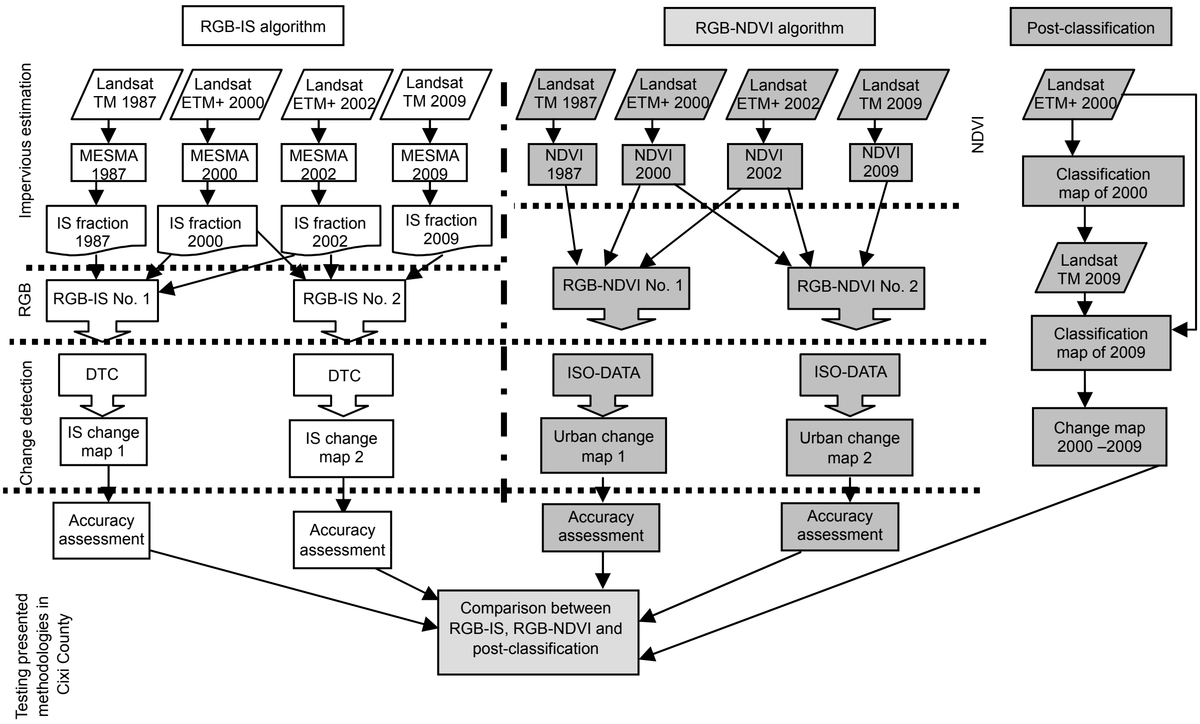

Fig. 2 Overview of methodologies (namely RGB-IS algorithm, RGB-NDVI algorithm, and post-classification)

Table 1 Summary of basic properties of the satellite imageries used

Date	Type of image	Spatial resolution (m)	Number of bands
May 18, 1987	TM 5	30	6
June 14, 2000	ETM+ 7	30	6
Nov. 11, 2002	ETM+ 7	30	6
Oct. 10, 2009	TM 5	30	6

Thermal and panchromatic images were not used in this study

other, more complex computational methods requiring ancillary data that were not available for this study (Song *et al*., 2001). Detailed descriptions of the dark object correction method are available in (Chaveze, 1996; Jensen, 2007).

3.2 Estimating impervious surface

SMA is based on the assumption that the reflectance $R_{i,\mathrm{b}}$ measured at pixel i for a given band of sensor (e.g., TM 1) can be modeled as the linear sum of N endmembers, or spectrally 'pure' materials, weighted by the fraction f_k of each endmember within the field of view of pixel (Powell *et al*., 2007). The SMA formula is

$$R_{i,\mathrm{b}} = \sum_{k=1}^{N} f_k R_{k,\mathrm{b}} + e_\mathrm{b}, \tag{1}$$

where e_b is the un-modeled residual. The traditional SMA uses a fixed number of endmembers to map the entire landscape. As a result, it cannot adequately capture the high spectral heterogeneity of urban materials. A technique that addresses these limitations is the MESMA, which allows the number and type of endmembers to vary per pixel (Roberts *et al*., 1998).

In the MESMA, endmember selection is a key step, and many techniques such as field investigation, lab analysis, and image selection are used. In practice, however, image based endmember selection methods are frequently used, because image endmembers can be easily obtained and they represent the spectral measured at the same scale as the image data (Lu and Weng, 2006). In this study, MESMA was started by selecting three endmembers, namely impervious surface, soil, and vegetation cover from Landsat images in 1987, 2000, 2002, and 2009.

The next step in MESMA was to remove spectra that had a high probability of confusion with other material classes and to identify which spectral were most representative of the spectral with their material class. To meet this demand, the EMC technique was used. EMC is an acronym for the three optimization techniques: endmember average root mean square error (EAR), minimum average spectral angle (MASA), and count based selection (CoB). In this regard, the optimum spectrum of each endmember had the highest CoB, lowest EAR, and lowest MASA. Also, this spectrum was most representative of the spectrum with its endmember.

In the third step, a range of SMA models (multi SMA models) were applied on the basis of the above spectrum. These models mapped each pixel in the image in terms of fractional abundance of land cover components in the image at a given point of time. Accordingly, three fraction images (impervious surface, soil, and vegetation) were produced by optimal models for each Landsat image. In this study, impervious surface fraction images were used to execute urban change analysis. After modeling, the performance of impervious surface fractions was evaluated by root mean square error (RMSE) and fraction value. The RMSE constraint is most commonly accepted in MESMA (Powell *et al.*, 2007). The results showed RMSE of most impervious surface pixels are less than 0.025 and fraction values range between −0.05 to 1.05. These pixels (unmixed pixels) were mainly located in the urban regions (Fig. 3, p.152). The rest of pixels included either RMSE values higher than 0.025 or non-reasonable fraction values, which were placed outside of urban regions.

Further information can be found in (Rashed *et al.*, 2003; Powell *et al.*, 2007; Roberts *et al.*, 2007; Rashed, 2008) regarding the calculation of impervious surface based on the MESMA.

3.3 Change detection using multi-temporal RGB-IS

Remotely sensed images are usually monitored using the RGB color system. The RGB system is based on an additive color theory that different combinations of red, green, and blue colors produce a complementary color. Sader and Winne (1992) and Jensen (2007) indicated that by knowing the date of band coupled with each color write function memory, the colors can be interpreted to identify change or no-change events in an area of interest.

In this respect, impervious surface images in 1987, 2000, and 2002 were assigned to blue, red, and green colors, respectively, to build RGB-IS No. 1 (the first period). RGB-IS No. 2 (the second period) was produced by placing the 2000 impervious surface image in the blue image plane, the 2002 impervious surface image in the red image plane, and the 2009 impervious surface image in the green image plane. The DTC was conducted to automate the change detection and turn the three layer impervious surface stack into a thematic map. The DTC is one of the non-parametric classification approaches. The technique has a number of advantages over the maximum likelihood (ML) and artificial neural networks (ANNs) algorithms. For example, the DTC is computationally fast (trained quickly and rapid in execution), makes no statistical assumptions (in contrast to the ML), and can handle data that are represented on different measurement scales (Pal and Mather, 2003).

In this study, the DTC was carried out twice, once for RGB-IS No. 1 and once for RGB-IS No. 2. Note that different DTC patterns (rules) were examined to construct the main pattern of DTC. An appropriate pattern was selected based on information in each DTC file and guided by interpretation of RGB-IS images and color table of urban internal modification (Table 2). In this regard, four urban changes classes namely HHH, LHH, LLH, and HLH were selected (Table 2). DTC patterns were built by ENVI RSI version 3.6.

RGB-NDVI was performed based on Sader *et al.* (2003) guidelines. In this respect, the RGB-NDVI image was classified by the ISO-DATA classifier. The number of urban change classes in RGB-NDVI was the same as that of RGB-IS. Further information regarding constructing RGB-NDVI can be found in (Sader *et al.*, 2003). We should make a technical point herein concerning usage of NDVI in our research. In general, high NDVI (toward +1) and low NDVI (toward −1) reflect plant cover and non-vegetation such as urban, respectively. In our research, we inverted this index, i.e., low NDVI (−1) and high NDVI (+1) represented vegetation cover and urban land, respectively. Therefore, high NDVI (urban land) and low NDVI (vegetation cover) were shown by H and L, respectively.

Table 2 Interpretation of internal urban modification codes and major colors based on the additive color theory in three date RGB-IS images (RGB-IS 2000-2002-2009 as an example) (Sader and Winne, 1992)

Major color	Impervious surface date			Type of change	Interpretation of change	Location
	2000	2002	2009			
	Blue	Red	Green			
White	H	H	H	–	Steady change	Urban center, transportation network
Yellow	L	H	H	Within-class	Development after 2000	Mainly urban center
Green	L	L	H	Between-class	Development after 2002	Rural land, sub urban and urban fringe, transportation network
Cyan	H	L	H	Within-class	Decreasing (2000–2002) and development (2002–2009)	Urban center

Note that most of the previous researches concerning RGB-NDVI were based on unsupervised classification technique and showed promising results (Sader and Winne, 1992; Sader *et al*., 2001; 2003). Therefore, we did not make any change in the structure of RGB-NDVI. However, for extracting urban change classes from RGB-IS images, the DTC was conducted. This is because, since the histogram of the features of interest in the urban area is often not normally distributed (Lu and Weng, 2005), unsupervised classifiers may not be very suitable for RGB-IS.

3.4 Post-classification

The post-classification method was also conducted to compare results of this technique with RGB-IS. For the post-classification, two thematic maps were derived by using the ML classifier from Landsat TM in 1987 and Landsat TM in 2009. In this case, four classes including urban, bare land, open land, and farm land were selected. Then two maps were compared on a pixel-by-pixel basis using change detection matrix for producing change map.

3.5 Accuracy assessment

An error matrix was conducted to assess the result of each classification, with which pertinent accuracy assessment parameters were derived. A total of 300 sampling points were randomly selected and examined, by using Landsat false color composite. The overall accuracy, producer's accuracy, user's accuracy, and the κ coefficient were calculated for each classified image.

4 Results and discussion

4.1 Qualification of RGB-IS, RGB-NDVI, and post-classification by visual interpretation

Impervious surface images of Cixi County for 1987, 2000, and 2002 were placed chronologically into the blue, red, and green color displays (Fig. 4a). This process was also repeated for 2000, 2002, and 2009 impervious surface images. Table 2 provides color interpretation of RGB-IS images. The resulting map displayed a range of colors that indicated the direction and magnitude of change in urban regions (Fig. 4a). For instance, green pixels were created by a combination of non-impervious surface pixels at date 1 (2000), non-impervious surface pixels at date 2 (2002) and impervious surface pixels at date 3 (2009). This color showed only one type of change and represented between-class changes. For example, non-impervious surface in 2000 and 2002 changed to impervious surface in 2009. Yellow pixels were an example of more than one kind of change and within-class change, in which the non-impervious surface in 2000 was changed to the low impervious surface in 2002. Then these areas were replaced by a high impervious surface (e.g., business district) in 2009 (Fig. 4a).

RGB technique was also applied to NDVI images for 1987, 2000, 2002, and 2009, and one example is given in Fig. 4b. In RGB-NDVI, decreasing NDVI value at three dates indicated urban expansion, which was represented by olive green to black color (Fig. 4b). These pixels in RGB-NDVI exhibited only one major vector change such as transition of non-urban areas observed in 2000 into urban areas in 2002 and 2009. RGB-NDVI images could not clearly identify urban changes, in comparison to RGB-IS. Also, we could not accurately define the color table of urban changes based on the RGB-NDVI.

Moreover, we used post-classification technique based on two images, including Landsat ETM 2000 and TM 2009 (Fig. 4). Although the result of this technique described the overall land cover change, it could not provide accurate measurement on pattern of urban changes regarding within-class change since it neglected impervious surface modification at the sub-pixel level. This technique also employed only two layers.

RGB-IS was sensitive to the sequence of increasing urban infrastructure and buildings, such as road networks, in comparison to RGB-NDVI (Fig. 5).

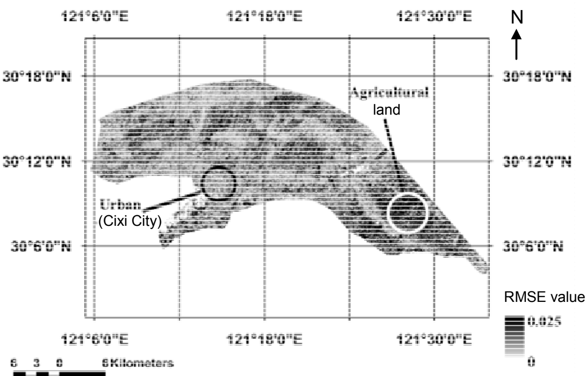

Fig. 3 RMSE map of MESMA models for Landsat ETM 2002. High and low RMSE are in agricultural area and urban region, respectively

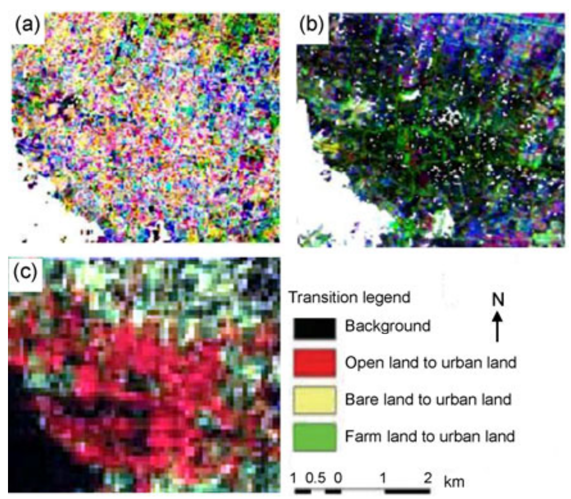

Fig. 4 A comparison between RGB-IS 2000-2002-2009 (a), RGB-NDVI 2000-2002-2009 (b), and transition map (c) produced by post-classification for the south east part of Cixi County

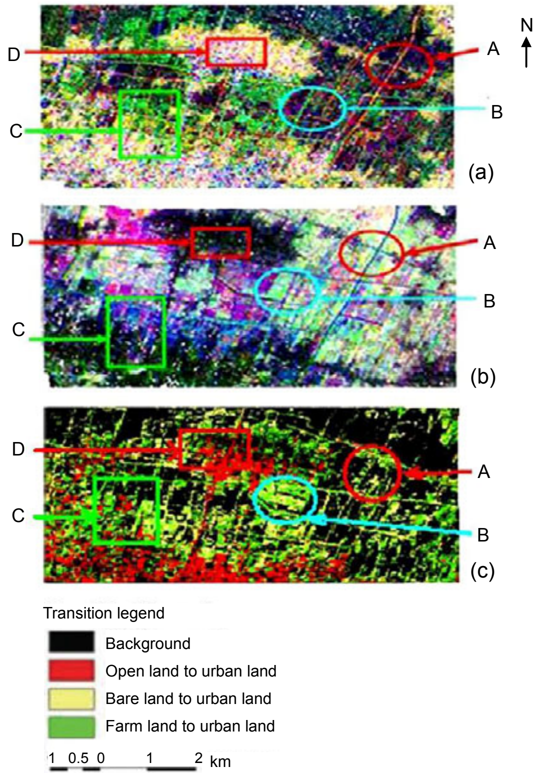

Fig. 5 RGB-IS 2000-2002-2009 (a), RGB-NDVI 2000-2002-2009 (b), and transition map (c) resulted from post-classification

A and B indicate roads constructed before 2000 and after 2002, respectively, and C and D represent locations of between-class change (suburb) and within-class change (urban center), respectively

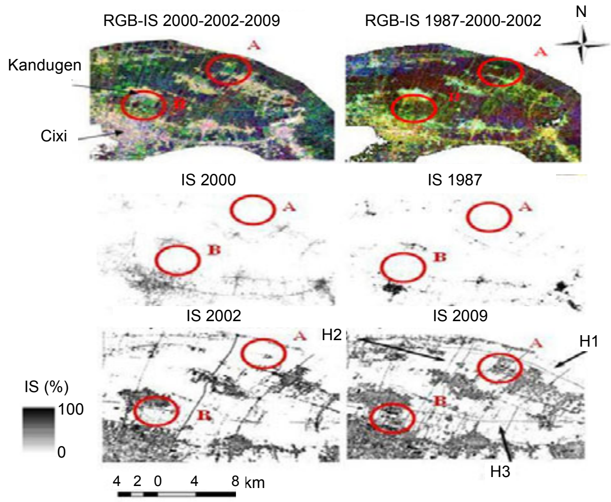

Fig. 7 Sequence of impervious growth along highways (a) and around suburb (b)

H1: Shenhai Expressway (Hangzhou Bridge Highway); H2: Zhangxi North Highway; H3: Zhongheng Line; IS: impervious surface

For example, in RGB-IS 2000-2002-2009, some roads indicated by the red color suggested that they were constructed before 2000 (Fig. 5a). This was because these roads were presented on all the Landsat images. Roads constructed between 2002 and 2009 were depicted by the green color because they were not in TM 1987, ETM 2000, and ETM 2002 (Fig. 5a). Also, two types of change were detected in urban regions. The urban centers showed within-class change or increasing percentage of imperviousness index (e.g., low density urban area change to high density urban area), which was represented by two major colors, namely, cyan and yellow colors. By contrast, suburban areas and along highways showed between-class changes or expansion of impervious surface (non-impervious surface transformed to urban land). This change was illustrated by green colors. However, although the roads and suburbs were present in RGB-NDVI images, they were drawn in different black color ranges. This made it difficult to extract the building sequence (Fig. 5b). Also, the output of post-classification (Fig. 5c) could not provide any information concerning internal modification of urban area, and detection of sequence of road networks as well.

4.2 Validating RGB-IS and RGB-NDVI through change/no change map

RGB-NDVI and RGB-IS images were classified to derive change and no-change maps in urban regions. The accuracy assessment was measured using error matrices built from 300 stratified-random samples, which were selected from the classified images and compared with Landsat color composite images in 1987, 2000, 2002, and 2009.

Table 3 provided a comparison of accuracy assessment results between the DTC and ISO-DATA classifiers that were used to classify RGB-IS and RGB-NDVI images, respectively. An overall accuracy of 83.33% and 77.33% were achieved in the classification results of RGB-IS 1987-2000-2002 and RGB-IS 2000-2002-2009, respectively. The LHH, LLH, and HHH had higher accuracies (greater than 71.93% of producer accuracy and 52.86% of user accuracy). The main confusion was mainly associated with the following pair of land change classes: HLH and LHH. This is because DTC could not accurately classify decreasing and increasing imperviousness for these classes. For instance, according to our definition, if imperviousness percentages for dates 2000, 2002, and 2009 were 30%, 29%, and 50%, respectively, the class change would be HLH; however, DTC classified this change as LHH.

The classification of the RGB-NDVI images with the ISO-DATA classifier yielded results that were much poorer than those which had been achieved in RGB-IS experiments (Table 3). This was predictable to a certain extent, because vegetation indices such as NDVI and reflected vegetation activity did not represent the surface conditions of the urban area directly (Kawamura *et al*., 1997), especially those sometimes causing similar reflection in urban areas (Cibula *et al*., 1992; Gao, 1996). Although NDVI is sensitive to the presence of green vegetation and commonly used to classify vegetation, the mixture of vegetation and other materials such as building, road, and parking lots in urban environments, particularly in sparse settlements, complicates

Table 3 Comparison between accuracy assessment results of RGB-IS and RGB-NDVI maps

Change type	RGB-IS No. 1 1987-2000-2002		RGB-IS No. 2 2000-2002-2009		RGB-NDVI No. 1 1987-2000-2002		RGB-NDVI No. 2 2000-2002-2009	
	PA (%)	UA (%)	PA (%)	UA (%)	PA (%)	UA (%)	PA (%)	UA (%)
LHH	87.01	93.06	77.78	73.68	71.62	53.00	75.00	72.86
HLH	92.50	52.86	95.74	64.29	–	–	–	–
HHH	92.75	88.89	73.97	75.00	90.70	78.00	88.71	81.75
LLH	71.93	95.35	71.30	93.90	58.39	80.00	72.22	34.67
Overall accuracy (%)	83.33		77.33		70.33		52.67	
Overall κ	0.77		0.69		0.55		0.38	

* HLH class could not be found in RGB-NDVI images; PA: producer's accuracy; UA: user's accuracy. We did not evaluate the accuracy of post-classification results, as the technique did not provide information concerning urban changes at the sub-pixel level

the use of NDVI (Setiawan *et al*., 2006). By contrast, impervious surface change investigation provided more information about the degree of urbanization and extent of urban land use (Fig. 6).

Fig. 6 illustrates impervious and NDVI changes over Cixi City, the capital of Cixi County in 1987, 2002, and 2009. As shown in Fig. 6a, impervious surface index captured and quantified within-class changes in land cover of Cixi City at the sub-pixel level. However, NDVI only showed homogeneity within a single pixel, resulting in no quantifiable change at the sub-pixel level. As a result, using conventional land change detection techniques such as combination of NDVI and ISO-DATA may result in a misleading conclusion about real changes in Cixi City. Furthermore, post-classification technique did not produce a continuous map for monitoring impervious surface changes at the sub-pixel level.

Another reason for the low accuracy assessment of RGB-NDVI may be attributed to the seasonal effects. Landsat images were not acquired on anniversary dates due to the monsoon climate of Hangzhou Bay (Ding *et al*., 2007), which made it difficult to obtain cloud-free images within the same year. However, impervious surface is stable and almost independent of seasonal changes and atmospheric conditions (Lu D. *et al*., 2006).

RGB-IS also confirmed the fact that integration of two or more classifiers yielded improved classification accuracy, compared to the use of a single classifier (Lu and Weng, 2007). In the present study, RGB-IS was a semi-hybrid classification technique, including MESMA and DTC, but RGB-NDVI and post-classification were only based on the unsupervised classification and supervised classification techniques, respectively. The accuracy chain of RGB-IS included several steps, namely finding optimum endmember model, selecting accurate DTC pattern, and final accuracy assessment, whereas only confusion matrix was conducted for RGB-NDVI and post-classification.

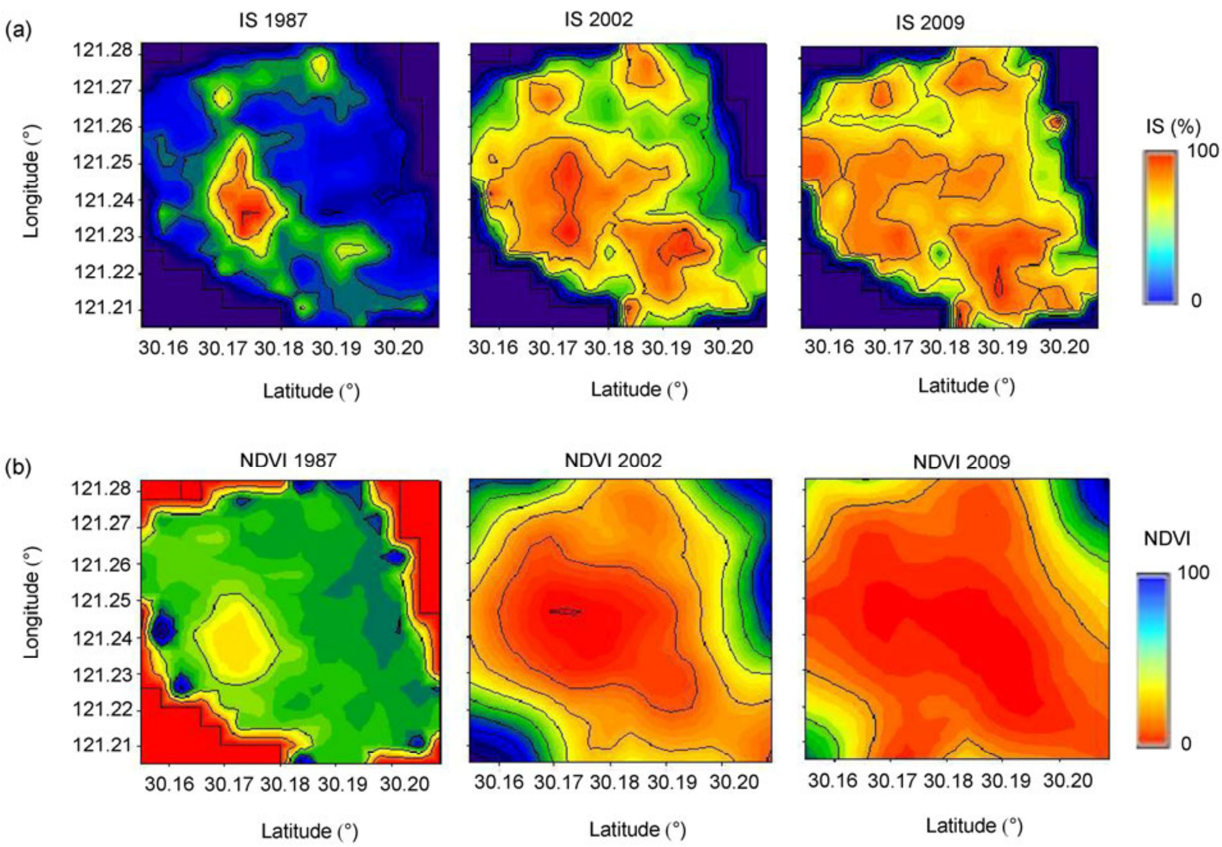

Fig. 6 A comparison between impervious surface (IS) (a) and NDVI (b) changes over Cixi City in 1987, 2002, and 2009
High value of IS (close to 100%) presents urban lands, while low value of NDVI (near to 0) shows urban lands

Although the results of RGB-IS were promising, compared to those of RGB-NDVI and post-classification, its accuracy was not yet to reach the level required by urban planners for practical application. Much of this low accuracy may be related to the environment of the study area, which was located in the coastal regions. Hence, there was a high degree of spectral confusion among sandy and urban regions. In addition, the morphology of urban regions in Cixi County was very dense. As a result, these situations may result in accurate differentiation between soil and impervious surface endmembers. Nevertheless, impervious surface performance in urban surface of highly heterogeneous nature is comparable with conventional methods (Powell *et al.*, 2007). However, more research is required to adapt this index for accurately mapping Chinese cities.

4.3 Testing RGB-IS in Cixi County to detect hotspot of growth

Visual inspection indicated that the spatial pattern of imperviousness estimation was quite reasonable for impervious surface maps in Cixi County. Urban centers, industrial zones, and highways were predicted with the highest imperviousness index (greater than 80%). Residential regions showed medium to high imperviousness (40%–70%). Areas of residential use around the urban-rural fringe were identified as low to medium imperviousness (25%–40%).

The result showed that Cixi County experienced a rapid urbanization from 1987 to 2009, which was witnessed by the significant increases of impervious surface. In this county, the magnitude of changes in urban land cover varied remarkably between the city center and its periphery. The urban center showed within-class changes (low impervious surface changed to high impervious surface) which were represented by red, yellow, and pink in RGB-IS images (Fig. 7, p.152). By contrast, urban periphery mostly showed between-class changes (non-impervious surface transformed to impervious surface) and this change was illustrated in cyan and green color in RGB-IS (Fig. 7, transect B over RGB-IS 2000-2002-2009).

There were two general forms of potential hotspot growth in Cixi County. Suburban areas were the first form of hotspot growth. The interesting point in Cixi County was conurbation phenomenon. In other words, continuous suburban expansion caused two or more than two cities to be connected together, leading to the formation of a big impervious area. This change was represented in the green color in RGB-IS images (Fig. 7). For instance, transect B showed a process of suburban expansion around Cixi City and Kandugen City (Fig. 7). By 1987 the mean of imperviousness for this region was 5%, while it increased to 45% in 2009.

Another growth hotspot was along the major transportation corridors. These regions were generally rural lands or small towns, which are surrounded by three to four highway networks. In this regard, an expanding area of impervious surface occurred during construction and operation of highways. The northeast of Cixi County was one clear example for this phenomenon (Fig. 7, transect A). This area is surrounded by three major transportation corridors, including Shenhai Expressway (Hangzhou Bridge Highway) in the north and east, Zhongheng Line in the south, and Zhangxi North Highway in the west. It is noteworthy that all these corridors were constructed between 2001 and 2008.

5 Conclusions

Changes in the imperviousness over time appear to be a useful indicator for identification of the spatial extent, intensity, and potentially, type of urban land cover/use changes (Yang *et al.*, 2003b). The present study tested three change detection techniques, namely RGB-NDVI, RGB-IS, and post-classification for monitoring impervious surface changes.

The results showed that RGB-IS provided more information about the degree of urbanization and proportion of urban lands, in comparison to RGB-NDVI and post-classification. Another advantage for applying RGB-IS in urban research was that the impervious surface was stable, and almost independent of seasonal changes and atmospheric conditions. Our investigation also showed that RGB-IS can be a valuable alternative for rapid and efficient mapping of hotspot growth and monitoring associated imperviousness changes.

Consequently, future research will increase the accuracy of urban change detection based on impervious surface fraction, rather than vegetation indices. However, it should further improve the present methodology, including (1) techniques for evaluating different impervious surface estimations which are appropriate for change patterns of Chinese cities, (2) examining other DTC methods to extract more accurate urban land change classes, and (3) testing the methodology developed herein by different satellite images in different regions to assess the generality of this technique.

Acknowledgements

The authors wish to thank Prof. Long-bin HUANG from University of Queensland, USA, Shan-shan WAN from Zhejiang University, China, and Golanze SHAHTAHMASSEBI from Plymouth University, UK for their comments and modifications.

References

Arnold, C.L., Gibbons, C.J., 1996. Impervious surface coverage: the emergence of a key environmental indicator. *Journal of the American Planning Association*, **62**(2): 243-258. [doi:10.1080/01944369608975688]

Cibula, W.G., Zetka, E.F., Rickman, D.L., 1992. Response of thematic bands to plant water stress. *International Journal of Remote Sensing*, **13**(10):1869-1880. [doi:10.1080/01431169208904236]

Chavez, P.S., 1996. Image-based atmospheric corrections—revisited and improved. *Photogrammetric Engineering and Remote Sensing*, **62**(9):1025-1036.

Chormanski, J., de Voorde, T.V., de Roeck, T., Batelaan, O., Canters, F., 2008. Improving distributed runoff prediction in urbanized catchments with remote sensing based estimates of impervious surface cover. *Sensors*, **8**(2): 910-932. [doi:10.3390/s8020910]

Deng, J.S., Wang, K., Hong, Y., Qi, J.G., 2009. Spatio-temporal dynamics and evolution of land use change and landscape pattern in response to rapid urbanization. *Landscape and Urban Planning*, **94**(3-4):187-198. [doi:10.1016/j.landurbplan.2009.05.001]

Ding, H., Wang, R.C., Wu, J.P., Zhou, B., Shi, Z., Ding, L.X., 2007. Quantifying land use change in Zhejiang coastal region, China using multi-temporal Landsat TM/ETM+ images. *Pedosphere*, **17**(6):712-720. [doi:10.1016/S1002-0160(07)60086-1]

Dougherty, M., Dymond, R.L., Goetz, S.J., Jzntz, C.A., Goulet, N., 2004. Evaluation of impervious surface estimates in a rapidly urbanizing watershed. *Photogrammetric Engineering and Remote Sensing*, **27**(11):1275-1284.

Esch, T., Himmler, V., Schorcht, G., Thiel, M., Wehrmann, T., Bachofer, F., Conrad, C., 2009. Large-area assessment of impervious surface based on integrated analysis of single-date Landsat-7 images and geospatial vector data. *Remote Sensing of Environment*, **113**(8):1678-1690. [doi:10.1016/j.rse.2009.03.012]

Franke, J., Roberts, D.A., Halligan, K., Menz, G., 2009. Hierarchical multiple endmember spectral mixture analysis (MESMA) of hyperspectral imagery for urban environments. *Remote Sensing of Environment*, **113**(8): 1712-1723. [doi:10.1016/j.rse.2009.03.018]

Gao, B.C., 1996. NDWI–a normalized difference water index for remote sensing of vegetation liquid water from space. *Remote Sensing of Environment*, **58**(3):257-266. [doi:10.1016/S0034-4257(96)00067-3]

Hu, X., Weng, Q., 2009. Estimating impervious surfaces from medium spatial resolution imagery using the self-organizing map and multi-layer perceptron neural networks. *Remote Sensing of Environment*, **113**(10): 2089-2102. [doi:10.1016/j.rse.2009.05.014]

Jensen, J.R., 2007. Introductory Digital Image Processing. Science Press and Pearson Education Asia Ltd., Beijing, China, p.127-173, 220-221.

Kawamura, M., Jayanmanna, S., Tsujiko, Y., 1997. Quantitative evaluation of urbanization in developing countries using satellite data. *Journal of Environmental System and Engineering*, **580**(5):45-54.

Klein, R., 1979. Urbanization and stream quality impairment. *Water Resources Bulletin*, **15**(4):948-963.

Lee, S., Lathrop, R.G., 2006. Subpixel analysis of Landsat ETM+ using self-organizing map (SOM) neural networks for urban land cover characterization. *IEEE Transactions on Geoscience and Remote Sensing*, **44**(6):1642-1654. [doi:10.1109/TGRS.2006.869984]

Li, C.L., Du, J.K., Su, Y.P., Li, Q., Chen, L., 2010. Extraction of Impervious Surface Based on Multi-Source Satellite Data of Qinhuai River Basin from 1979–2009. 18th International Conference on Geoinformatics, Beijing, China. [doi:10.1109/GEOINFORMATICS.2010.5567980]

Lizarazo, I., Barros, J., 2010. Fuzzy image segmentation for urban land-cover classification. *Photogrammetric Engineering and Remote Sensing*, **76**(2):151-162.

Long, H.L., Tang, G.P., Li, X.B., Heilig, G.K., 2007. Socio-economic driving forces of land-use change in Kunshan, the Yangtze River Delta economic area of China. *Journal of Environmental Management*, **83**(3): 351-364. [doi:10.1016/j.jenvman.2006.04.003]

Lu, D., Weng, Q., 2005. Urban classification using full spectral information of Landsat ETM+ imagery in Marion County, Indiana. *Photogrammetric Engineering and Remote Sensing*, **71**(11):1275-1284.

Lu, D., Weng, Q., 2006. Spectral mixture analysis of ASTER images for examining the relationship between urban thermal features and biophysical descriptors in Indianapolis, Indiana, USA. *Remote Sensing of Environment*, **104**(2):157-167. [doi:10.1016/j.rse.2005.11.015]

Lu, D., Weng, Q., 2007. A survey of image classification methods and techniques for improving classification performance. *International Journal of Remote Sensing*, **28**(5):823-870. [doi:10.1080/01431160600746456]

Lu, D., Weng, Q., Li, G., 2006. Residential population estimation using a remote sensing derived impervious surface approach. *International Journal of Remote Sensing*, **27**(16):3553-3570. [doi:10.1080/01431160600617202]

Lu, S.L., Shen, X.H., Zou, L.J., 2006. Land cover change in Ningbo and its surrounding area of Zhejiang Province, 1987~2000. *Journal of Zhejiang University-SCIENCE A*, **7**(4):633-640. [doi:10.1631/jzus.2006.A0633]

Luo, L., Mountrakis, G., 2010. Integrating intermediate inputs from partially classified images within a hybrid classification framework: An impervious surface estimation example. *Remote Sensing of Environment*, **114**(6): 1220-1229. [doi:10.1016/j.rse.2010.01.008]

Mountrakis, G., Luo, L., 2011. Enhancing and replacing spectral information with intermediate structural inputs: A case study on impervious surface detection. *Remote Sensing of Environment*, **115**(5):1162-1170. [doi:10.1016/j.rse.2010.12.018]

Mountrakis, G., Watts, R., Luo, L., Wang, J., 2009. Developing collaborative classifiers using an expert-based model. *Photogrammetric Engineering and Remote Sensing*, **75**(7):831-844.

Pal, M., Mather, M.P., 2003. An assessment of the effectiveness of decision tree methods for land cover classification. *Remote Sensing of Environment*, **86**(4):554-565. [doi:10.1016/S0034-4257(03)00132-9]

Powell, R.L., Roberts, D.A., Dennison, P.E., Hess, L.L., 2007. Sub-pixel mapping of urban land cover using multiple endmember spectral mixture analysis: Manaus, Brazil. *Remote Sensing of Environment*, **106**(2):253-267. [doi:10.1016/j.rse.2006.09.005]

Powell, S.L., Cohen, W.B., Yang, Z., Pierce, J.D., Alberti, M., 2008. Quantification of impervious surface in Snohomish water resource inventory area of western Washington from 1972–2006. *Remote Sensing of Environment*, **112**(4):1895-1908. [doi:10.1016/j.rse.2007.09.010]

Ramadan, E., Feng, X.Z., Cheng, Z., 2004. Satellite remote sensing for urban growth assessment in Shaoxing City, Zhejiang Province. *Journal of Zhejiang University SCIENCE*, **5**(9):1095-1101. [doi:10.1631/jzus.2004.1095]

Rashed, T., 2008. Remote sensing of within-class in urban neighborhood structures. *Computers, Environment and Urban Systems*, **32**(5):343-354. [doi:10.1016/j.compenvurbsys.2008.06.007]

Rashed, T., Weeks, J., Roberts, D.A., Rogan, J., Powell, P., 2003. Measuring the physical composition of urban morphology using multiple endmember spectral mixture models. *Photogrammetric Engineering and Remote Sensing*, **69**(9):1011-1020.

Rashed, T., Weeks, J.R., Stow, D., Fugate, D., 2005. Measuring temporal compositions of urban morphology through spectral mixture analysis: toward a soft approach to change analysis in crowded cities. *International Journal of Remote Sensing*, **26**(4):699-718. [doi:10.1080/01431160512331316874]

Roberts, D.A., Gardner, M., Church, R., Ustin, S., Scheer, G., Green, R.O., 1998. Mapping chaparral in the Santa Monica Mountains using multiple endmember spectral mixture models. *Remote Sensing of Environment*, **65**(3): 267-279. [doi:10.1016/S0034-4257(98)00037-6]

Roberts, D., Halligan, K., Dennison, P., 2007. Vipers Tools User Manual. Available from http://www.vipertools.org/?q=content/envi-plugin-0 [Accessed on Apr. 21, 2011].

Sader, S.A., Winne, J.C., 1992. RGB-NDVI colour composites for visualizing forest change dynamics. *International Journal of Remote Sensing*, **13**(16):3055-3067. [doi:10.1080/01431169208904102]

Sader, S.A., Hayes, D.J., Hepinstall, J.A., Coan, M., Soza, C., 2001. Forest change monitoring of a remote biosphere reserve. *International Journal of Remote Sensing*, **22**(10): 1937-1950. [doi:10.1080/01431160117141]

Sader, S.A., Bertrand, M., Wilson, E.H., 2003. Satellite change detection of forest harvest pattern on an industrial forest landscape. *Forest Science*, **49**(3):341-353.

Setiawan, H., Mathieu, R., Thompson-Fawcett, M., 2006. Assessing the applicability of the V-I-S model to map urban land use in the developing world: Case study of Yogyakarta, Indonesia. *Computers, Environment and Urban Systems*, **30**(4):503-522. [doi:10.1016/j.compenvurbsys.2005.04.003]

Small, C., 2005. A global analysis of urban reflectance. *International Journal of Remote Sensing*, **26**(4):661-681. [doi:10.1080/01431160310001654950]

Song, C., Woodcock, C.E., Seto, K.C., Lenney, M.P., Macomber, S.A., 2001. Classification and change detection using Landsat TM data: when and how to correct atmospheric effects. *Remote Sensing of Environment*, **75**(2):230-244. [doi:10.1016/S0034-4257(00)00169-3]

Weng, Q., 2007. Remote Sensing of Impervious Surfaces. CRC Press, Boca Raton, Florida.

Yang, X., 2006. Estimating landscape imperviousness index from satellite imagery. *IEEE Geosceince and Remote Sensing Letters*, **3**(1):6-9. [doi:10.1109/LGRS.2005.853929]

Yang, X., Liu, Z., 2005. Use of satellite-derived landscape imperviousness index to characterize urban spatial growth. *Computers, Environment and Urban Systems*, **29**(5):524-540. [doi:10.1016/j.compenvurbsys.2005.01.005]

Yang, L., Huang, C., Homer, C.G., Wylie, B.K., Coan, M.J., 2003a. An approach for mapping large-area impervious surfaces: Synergistic use of Landsat-7 ETM+ and high spatial resolution imagery. *Canadian Journal of Remote Sensing*, **29**(2):230-240. [doi:10.5589/m02-098]

Yang, L., Xian, G., Kalver, J.M., Deal, B., 2003b. Urban land-cover change detection through sub-pixel imperviousness mapping using remotely sensed data. *Photogrammetric Engineering and Remote Sensing*, **69**(9):1003-1010.